



---

## Chimney Backflow Effect on House with Improved Cook Stove in Rural Mountainous Region of Nepal

Indira Parajuli\*, Heekwan Lee

School of Urban and Environmental Engineering, Incheon National University, 406-772, 119, Academy Street, Yeonsu-gu, Incheon, Republic of Korea

---

**Abstract** Indoor Air Quality (IAQ) in rural households, particularly in a single cell house (SCH), is a crucial issue while dwellers' cooked with solid fuel. IAQ is affected by many factors such as firewood moisture contains, stove types, chimney orientation, and height, etc. This study has focuse don the IAQ situation and the backflow effect. Indoor Air Pollution (IAP) monitoring is carried out in two adjoining remote villages of Palpa District of Western Nepal. Computational fluid dynamics (CFD) modeling is applied to carry out backflow modeling using the inventory data derived from the field study.

The mean Carbon monoxide (CO) and PM<sub>2.5</sub> concentration for improved cook stove (ICS) is 27.11ppm and 825.4  $\mu\text{g}/\text{m}^3$  ( $27.11 \pm 14.24$  ppm and  $825.4 \pm 730.9$   $\mu\text{g}/\text{m}^3$ ) with significant relation ( $p < 0.0001$ ). Almost sampled households have pollution concentration exceeding the guidelines value due to the effect of backflow. Placement of chimney at short height is found to be a major cause of backflow. The smoke comes out from indoor space at low height reenters into the house due to high turbulence intensity (TI) i.e. 68% on leeward side while air flow from front to back part of the house and 20% while airflow from back to a front part of the house. TI is increased with increase in building height influencing up to 3m vertical height. This indicates that minimal height of the chimney outlet opening should be placed above 3m height to prevent backflow to the indoor space. Low pressure on a leeward side of a house at the height of 1m forms a cavity or eddy or vortices zones allowing airback along with smoke into the house again. Hence, this study recommends to greater focus on chimney orientation and height to control IAQ in an SCH.

**Keywords** Carbon Monoxide, Particulate Matter, Single Cell House, Indoor Air Quality, Backflow Effect, CFD Modeling.

---

### 1. Introduction

Around 78% households in Nepal are still solely relying on solid biomass fuels for cooking and space heating purposes [27]. Cooking and heating with solid fuels on open fires result in high concentration of IAP. Indoor smoke contains a high range of health-damaging pollutants such as PM<sub>2.5</sub>, CO, etc. indoor smoke exceeds acceptable concentration for total suspended particles (TSP) accounting more than 100 folds in a poorly ventilated kitchen [12]. The concentration of IAPs originating from the burning of solid fuels depends on a number of factors such as fuel type, characteristics of housing and methods of cooking, height and orientation of chimney. The extent of pollutants can vary from day to day and within the day depending on cooking activities [15]. The mean personal exposure to CO in TCS and ICS are 380ppm and 67ppm, respectively. It implies that ICS reduces indoor TSP and CO concentration by 71% and 82% respectively [3], [22], [7].

These stoves significantly reduce fuel consumption and harmful emissions in the kitchen. However, the adoption of ICS has proved to be difficult [33], [24]. Many implemented projects all over the world have faced



low adoption rates. Even those programs claiming of high adoption rates are found to be uncertain of the impact of the ICS in IAQ, health and fuel consumption of the beneficiaries [17], [19], [29].

Various ICS have been developed and promoted by the National and International agencies for the sake of reduction of the IAP. ICS is introduced in Nepal in the 1950s and continues to be relevant in the present context. The governmental, non-government and private organizations are involved in developing and promoting different types of ICS in Nepal. More than 700,000 improved cook stoves have been installed in 63 districts [1]. Most of the mud ICS particularly in a context of Nepal has been promoted with a short chimney height i.e. 1.2m for the sake of extraction of the smoke from the indoor space. The external factors associated with the performance of the stove have not been taken into consideration while designing the stove. Although many households of Nepal have already utilized ICS, IAP concentration in Nepalese houses is much higher than the standard permissible value for safe health as prescribed by WHO and USEPA [14], [40].

The performance of wood stoves in fuel use reduction has mainly been assessed using experimental methods such as water boiling test (WBT) and controlled cooking test (CCT). However, these laboratory-based tests have not been able to reflect the real performance of cook stoves during daily cooking activities [6], [34] and [21]. A more representative method is the Kitchen Performance Test (KPT), a stove performance test that measures fuel use in households under actual use [34]. Very few studies have utilized this method to evaluate the performance of the cook stove. Therefore, people are exposing with a high concentration of pollutants into their houses up on their daily cooking practices. This is not only because of the stove performance but also due to the associated external factors like external wind direction and orientation of chimney. The problem of backflow in a low rising building is serious even though the houses with ICS because of the short stack height. Once smoke comes out from the stack at a low height, it reenters easily into the house recirculating around the building due to an effect of velocity gradient, pressure difference, and turbulence intensity (TI), etc.

As the flow approaches the building, it divides into four main streams; the first stream deviates over a building, the second stream has deviated down windward facade and other two streams deviated to two sides of building [26], [25]. At a point of deviation, a stagnation point is formed with maximum pressure situated at that point. The flow then changes the direction from the point to lower pressure zone of the facade; upwards, to sides and downwards. The air flows downward forming a standing vortex in front of windward facade corner streams. Various studies have shown that the pressure distribution along the leeward wall is almost uniform and below the atmospheric pressure [42]. The negative pressure distribution on a leeward roof near rear wall has the same magnitudes and they are stronger than a negative pressure on the windward roof except leading edge in case of 30° roof pitch. The recirculation regions decrease with increasing roof pitch. It is occurred in the leeward roof due to flow separation extending along the mixing layer. If there is the source of pollutants in low height then it easily reenters into the house causing indoor pollution concentration higher than the acceptable values.

This study has mainly focused on CO and PM<sub>2.5</sub> pollutants concentration in households with ICS and effect of backflow. A major objective of this study is to quantify the indoor pollutants concentration and determine the cause of high concentration with backflow modeling using the commercial software CFD. The result of this study will be helpful to prevent backflow due to chimney orientation and height. However, this paper has limitation about the technique of efficient ventilation, energy conservation, and efficient burning.

## 2. Materials and Methods

### 2.1. Study Site

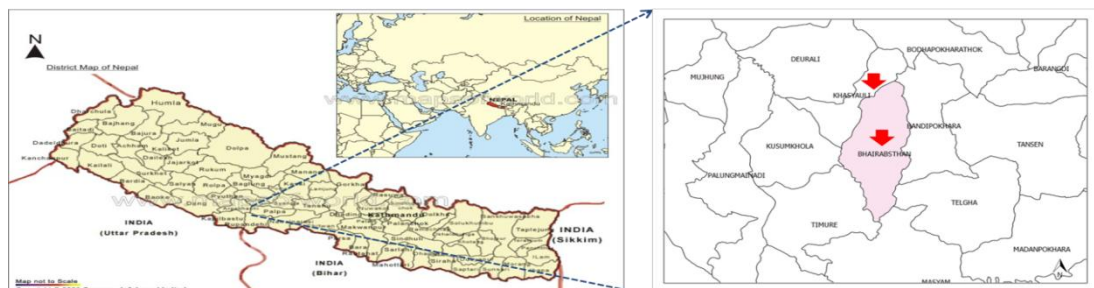


Figure 1: Geographical position of study area and specific location of study Site



The study is conducted in rural two VDCs: Khasauli and Bhairabsthan of Palpa ( $28^{\circ}40'N$   $83^{\circ}15'0''E$  with an altitude of 1838m, i.e. mid-hills with a temperate climate), district of western Nepal. Bhairabsthan VDC is situated 9km and Khasauli VDC is 11km away from Tansen (Headquarter of Palpa District). These VDCs are situated in the southeast of Tansen, 38km away from Siddhartha highway. The main source of cooking fuel in these areas is firewood collected from community forest. Even though a majority of the households in the areas have ICS rather than TCS, they are not in a well-functioning state due to backflow problem with short chimney height.

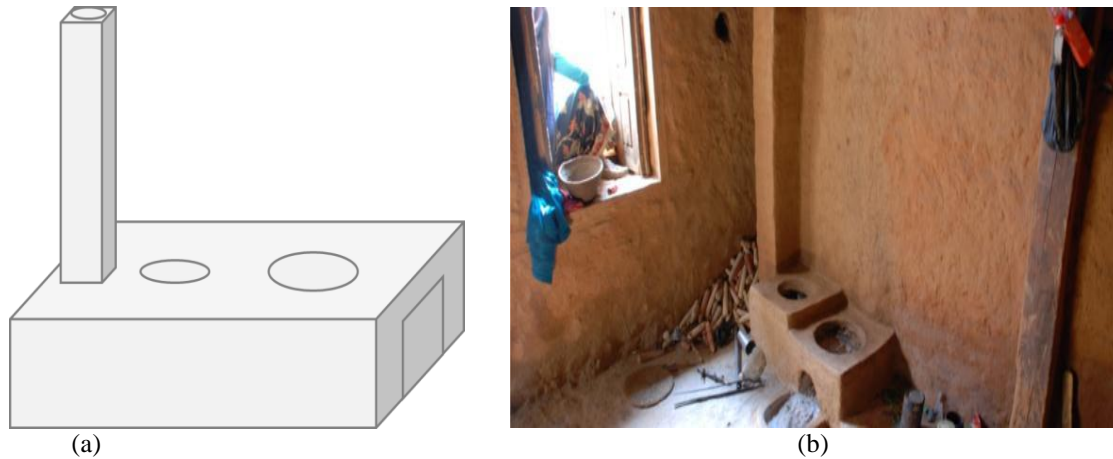


Figure 2: Solid fuel cook stoves (a) Improved Cook Stove model (ICS) (b) Mud improved Cookstoves having chimney outlet nearby back window

## 2.2. Indoor Air Pollution Monitoring

IAQ is assessed with continuous monitoring for 24h in a sampled household applying sampling protocol developed by Center for Entrepreneurship in International Health and Development (CEIHD), University of California, Berkeley. The main intend of monitoring is to assess daily stove used for preparing two major meals in the morning and evening and a short meal (fast food) in the afternoon in sampled household. CO and  $PM_{2.5}$  are considered as key IAPs arising from firewood burning, which are epidemiologically important indicators of IAP, WHO, 2005b [40]. Hence, concentrations of  $PM_{2.5}$  and CO are taken as an indicator of the IAP in this study.

## 2.3. House structure and orientation

Generally, houses are of single cell types having kitchen and living room within the same enclosure made from mud and stone wall with galvanized inclined ( $30^{\circ}$ ) iron sheet roof.

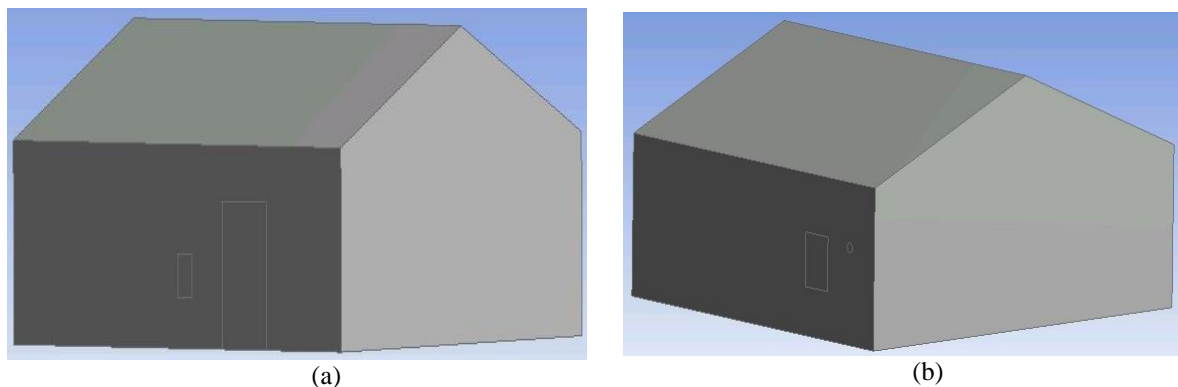


Figure 3: Structure of Single Cell House in a study area: (a) front part of house (b) back part of house



Generally, there are two windows one at the front part and other at the back part of the house as shown in Fig. 3. People usually burn firewood inside the enclosure. The houses with ICS have 1.2m height chimney attached with ICS as shown in Fig. 2. Chimney outlet part is generally placed at the back wall nearby back window opening. In the mountainous region, almost houses are facing towards South as in Fig. 3. Few of the houses are East facing.

#### 2.4. Backflow Modeling

The effect of backflow is caused by distortion of the airflow due to the obstruction of the house. While the wind blows near ground level that experiences friction between airflow and ground surface creating boundary layer called atmospheric boundary layer (ABL). ABL covers up to 1~2 km [4].

ABL domain dimension of  $X \times Y \times Z = 25\text{m} \times 25\text{m} \times 10\text{m}$  with an SCH having dimension  $5.5\text{m} \times 6\text{m} \times 2.5\text{m}$  inside the ABL domain is taken as a domain in this study. The meshing is used at equidistance with a spacing of 0.24m in X, Y and Z directions with tetrahedral cells having elements 661002 and nodes 118702. This is adopted as noted from Yang et al., 2009 and Dutton et al., 2005, asserted that the horizontal homogeneity of ABL profile is independent of mesh resolution. It has been noted that horizontal homogeneity of ABL profile is independent of mesh resolution [43], [13].

Simulation is performed using commercial CFD code fluent 13.0. The governing equations are written as follows, Versteeg, 1995 [37].

**Continuity equation:**

$$\frac{\partial}{\partial x_i} (u_i) = 0 \quad (1)$$

**Momentum equation:**

$$\frac{\partial}{\partial x_j} (\rho u_i u_j) = -\frac{\partial p}{\partial x_j} + \frac{\partial}{\partial x_j} \left[ \mu \left( \frac{\partial u_i}{\partial x_j} + \frac{\partial u_j}{\partial x_i} \right) - \overline{\rho u_i u_j} \right] \quad (2)$$

Where, the values of both i and j range from 1 to 3;  $u_i$  is the time average velocity and  $u_i'$  is fluctuating component;  $\rho$  is the mass density of air; p is the pressure;  $\mu$  is the turbulent viscosity;  $-\overline{\rho u_i u_j}$  is the Reynolds stress by Anderson, 1995; compared with the standard k- $\epsilon$  turbulent model, the RNG k- $\epsilon$  model is applied by Chunzi Nan et al., 2015 in study of air backflow effect in a ventilated tunnel [2], [5]. Hence, a similar model is applied in this study to draw the result of backflow of smoke into the house. The RNG k- $\epsilon$  the turbulent model can be represented as Versteeg, 1995; Wang, 2004 [37], [38].

**K-equation:**

$$\frac{\partial(\rho k u_i)}{\partial x_i} = \frac{\partial}{\partial x_j} \left[ \alpha_k \mu_{eff} \frac{\partial K}{\partial x_j} \right] + G_k - \rho \epsilon \quad (3)$$

**$\epsilon$  - Equation:**

$$\frac{\partial(\rho \epsilon u_i)}{\partial x_i} = \frac{\partial}{\partial x_j} \left[ \alpha_\epsilon \mu_{eff} \frac{\partial \epsilon}{\partial x_j} \right] + \frac{C_{1\epsilon}^* \epsilon}{K} G_k - C_{2\epsilon} \rho \frac{\epsilon^2}{k} \quad (4)$$



Where,  $G_k = \mu_t \left( \frac{\partial u_i}{\partial x_j} + \frac{\partial u_j}{\partial x_i} \right) \frac{\partial u_i}{\partial x_j}$   $\mu_t$  is the turbulent viscosity,  $\mu_{eff} = \mu + \mu_t$ ;  $\mu_t = \frac{\rho C_\mu k^2}{\varepsilon}$ ;  $C_\mu = 0.0845$ ;  $\alpha_k = 1.39$ ;  $C_{1\varepsilon}^* = C_{1\varepsilon} - \frac{\eta(1 - \eta/\eta_0)}{1 + \beta\eta^3}$ ;  $C_{1\varepsilon} = 1.42$ ;  $C_{2\varepsilon} = 1.68$ ;  $\eta = (2E_{ij} \cdot E_{ij})^{1/2} \frac{k}{\varepsilon}$ ;

$$E_{ij} = \frac{1}{2} \left( \frac{\partial u_i}{\partial x_j} + \frac{\partial u_j}{\partial x_i} \right); \eta_0 = 4.377; \beta = 0.012$$

The inlet boundary condition is calculated using the exponential formula (a power law relationship) as in equation (1) that derived vertical profile of wind velocity in boundary layer as shown in **Fig.4**.

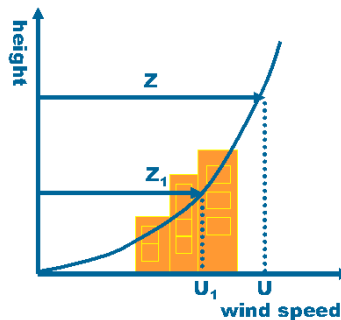


Figure 4: Vertical wind profile in the atmospheric boundary layer

The vertical wind velocity is expressed by the equation:

$$U = U_0 \left( \frac{z-d}{z_0} \right)^p \quad (5)$$

Where, U is the wind velocity (m/s) at corresponding height Z (m),  $U_0$  is wind velocity at reference height  $Z_0$  (=10m) and d is zero plane displacement height in meter above ground at which zero wind speed is achieved as a result of flow obstacles such as trees or buildings. P is constant representing roughness of ground surface which increases in value for increased roughness. The exponential p has typical values of 0.16 for open country terrain as recommended by Kato et al., 2009 [23].

#### Boundary conditions

- 1) Inlet boundary: vertical velocity profile is set using equation (1)
- 2) Outlet Boundary: pressure outlet boundary is adopted.

Top and side boundary conditions are specified as symmetry while outlet boundary conditions are specified as pressure outlet. Reynolds Average Navier–Stokes method (RANS) turbulent model is applied in a simulation.

### 3. Results and discussion

Both  $PM_{2.5}$  and CO are monitored in 10 households having ICS (n=10). Results show that indoor concentration is found exceeding the threshold value recommended by various organizations like WHO, USEPA for safe health. This is because of the observed impact of backflow which has been proved from backflow modeling result of this study.

#### 3.1. Status of IAP

The 12hours mean concentration of CO and 24hours mean concentration of  $PM_{2.5}$  are 27.11ppm and  $825.4\mu g/m^3$  respectively, with a confidence interval of 35.93 -18.28 with CO and 1278.42 - 372.38 with  $PM_{2.5}$ . The **Fig 5**



shows that CO and PM<sub>2.5</sub> concentration of households have a higher value than the WHO permissible value i.e. 8.732ppm and 25µg/m<sup>3</sup> respectively, with the confidence interval 21.58 -27.67 and 1278.42 - 372.38, respectively. The typical CO concentration of 12hours and PM<sub>2.5</sub> concentrations of 24hours sample period in the same household are peaked generally together as both pollutants are produced during combustion of firewood while cooking.

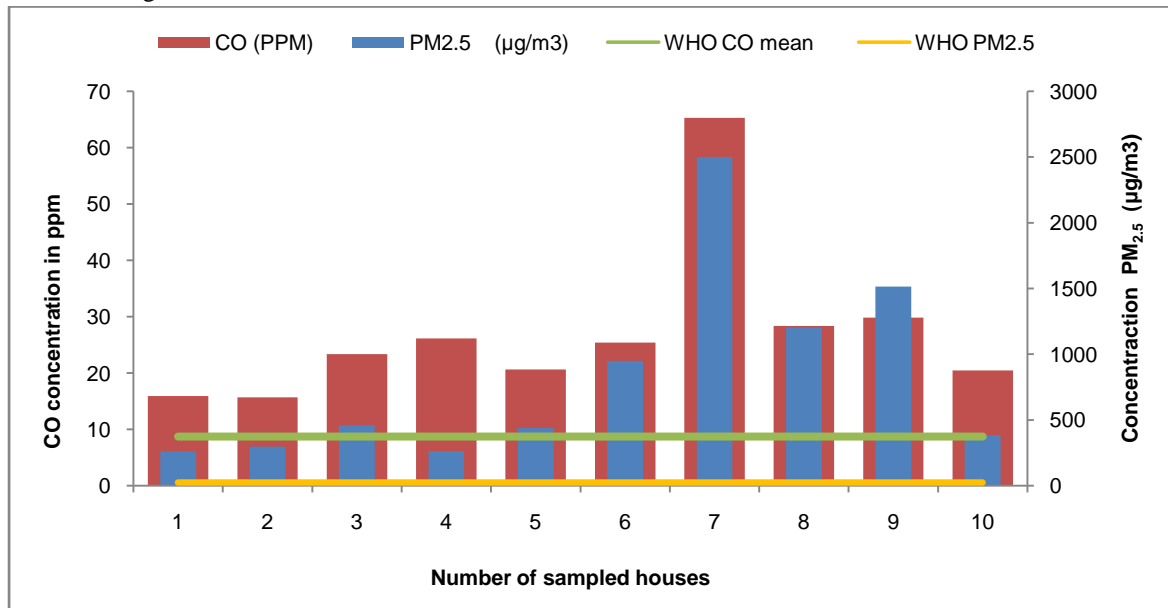


Figure 5: Comparison of CO and PM<sub>2.5</sub> concentration in ICS with WHO permissible value

The indoor environment is found harmful with ICS as the performance of Chimney is not efficient. This shows that small reduction in CO concentration is merely due to the changes in quality of fuel rather than the performance of chimney and ICS. A Recent study carried out by Aprovecho Research Center (ARC), USA [35] also shows that chimney stoves are less efficient as it lowers to boil and consumes more fuel. Further, IAPs concentration has not been lowered down as per permissible value. Therefore, invisible PM<sub>2.5</sub>, CO, and powerful climate forcing pollutants are still exceeding inside a rural household.

Table 1: Improved Cook stove 12hours CO and 24hours PM<sub>2.5</sub> concentration data comparison

Pollutants Type	8hours mean CO (ppm)								24hoursPM <sub>2.5</sub> (µg/m <sup>3</sup> )							
	Min	Max	Mean	Median	Mode	SD	Range	95% Confidence Interval (CI)	Min	Max	Mean	Median	Mode	SD	Range	95% Confidence Interval (CI)
ICS (n= 10)	13.69	30.91	24.63	24.15	13.69	4.91	17.22	21.5843-27.6757	259.6	2500	825.4	449.5	259.6	730.9	2240	1278.42-372.383

Table 2: Improved Cook stove 8hours CO and 24hours PM<sub>2.5</sub> concentration data comparison

Pollutants Type	ICS ( n= 10)							
	Mean	Median	Mode	SD	Min.	Max.	Range	95% Confidence Interval (CI)
CO (PPM)	27.11	24.37	15.7	14.24	15.7	65.27	49.57	35.936-18.284
PM <sub>2.5</sub> (µg/m <sup>3</sup> )	825.4	449.5	259.6	730.9	259.6	2500	2240	1278.42-372.383

### 3.2. Wind flow effect around house

#### 3.2.1. Air flow pattern

Pressure coefficient (C<sub>p</sub>) and non-dimensional velocity magnitude (|V|/U<sub>ref</sub>) are analyzed to show more detailed analysis of effect of inclined roof configuration on flow pattern around house. The pressure coefficient C<sub>p</sub> is calculated as follows:



$$C_p = \frac{(P - P_0)}{(0.5\rho U_{ref}^2)} \quad (6)$$

Where, P is static pressure,  $P_0$  the reference static pressure,  $\rho$  air density (=1.225 kg/m<sup>3</sup>: International Standard Atmosphere (ISA); dry air,  $P_0=101,325$  Pa (ISO 2533, 1975), and  $U_{ref}$  is the approach – flow wind speed at house height ( $U_{ref}=2.8$  m/s at  $z_{ref}=2.5$ m). Static pressure increase in front of house is caused by the larger blockage of flow by house with eaves and inclined roof, similar result is found in other studies [8], [9], [10], [11], [20], and [41]. Decrease in absolute value of static pressure behind building is due to change in flow rate in inclined roof as shown in **Fig. 6**. Pressure distribution on windward walls of house is positive due to pushing effect. Negative pressure fields occur both on roof and leeward walls of house due to flow separation from leading edges of roofs.  $C_p$  has minimum values near leading edge of roof and increases to maximum values and again decreases to windward edge. This behavior is due to recirculation region induced by flow separating from leading edge.  $C_p$  decreases on windward roof as well in rear wall as shown in **Fig.6(a)**. and **6(b)**. The Similar result is obtained in study done by Y. Ozmen et al., 2015 [42].

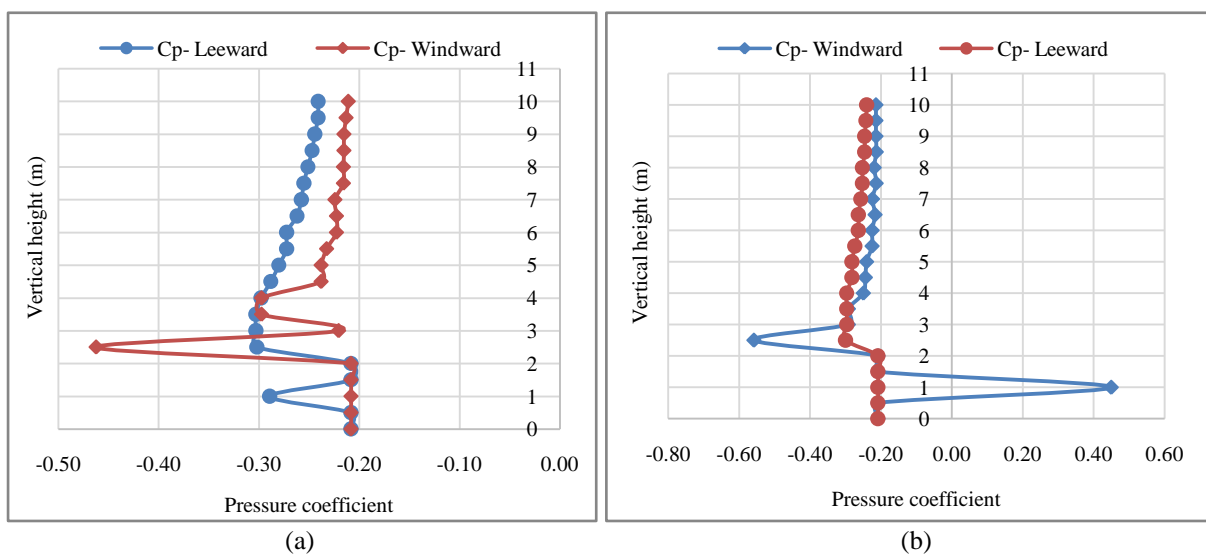


Figure 6: Pressure coefficient distribution at different vertical height: (a) Pressure coefficient at different points while wind flow from front part (b) Pressure coefficient at different location while wind flow from back part.

### 3.2.2. Backflow effect

With shorter chimney height and placement of chimney outlet nearby back window, smoke extracted out from the chimney easily reenters via adjoining window opening that is visible while surveying. The smoke came out from chimney due to buoyancy as a driving force; smoke easily turned back inside from the adjoining openings [28].

#### 3.2.2.1. Wind flow from front side of house

The CFD simulation result shows that once the wind flows from a front part of a house, air is blocked in front part due to high pressure and passing air towards lee side (back part of a house) with low pressure. The air moves towards back side due to a suction effect on back part caused by negative pressure or low pressure than that of a windward side as depicted in **Fig. 7(a)**, **7(b)**, **7(c)** and **7(d)**. At the same time while the smoke comes out from vent pipe below roof due to buoyancy driving force that spreads around and air reenters into the adjoining window opening. Thus, the extracted smoke reenters into the house in an unwanted concentration causing concentration higher than the safe value.



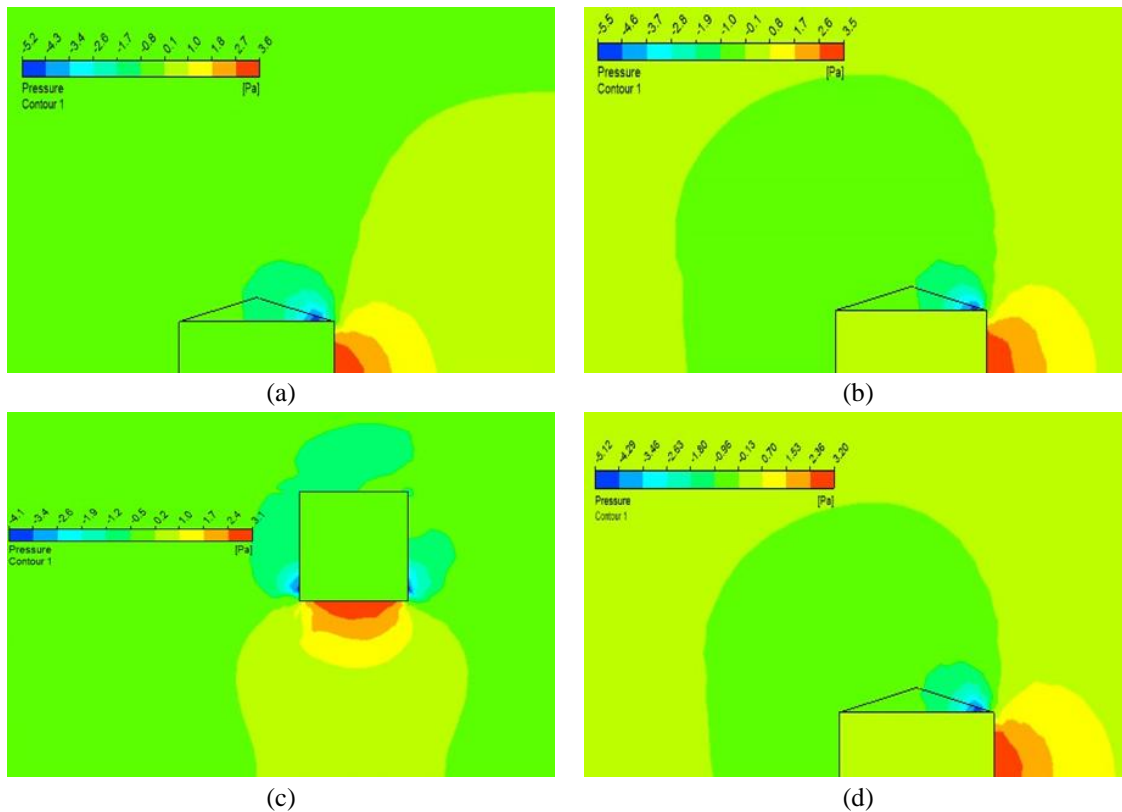


Figure 7: Air flow from front to back part of house: Pressure contour (a) YZ plane front window central plane (b) YZ plane front door central plane (c) XZ plane at chimney height plane (d) YZ back window central plane

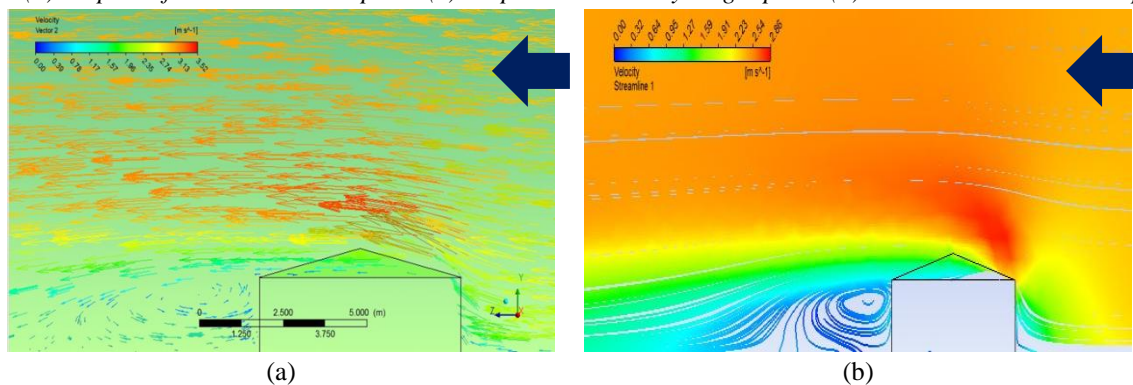


Figure 8: Air flow from front towards back side of house: (a) Velocity vector YZ plane front window central plane (b) streamline velocity YZ plane central plane

Vortex formation starts on windward direction and extends along its side and roof then finally moves towards leeward side of the house. The deviation from main stream takes place at point of maximum pressure on windward facade of house. The flow gets separated due to wall but is reattached again in leeward direction of the house. Similarly, flow is separated while hitting windward edge of wall reattaching again on the top of the roof. In such a separation and reattachment of flow, recirculation areas are formed called eddies or vortices (conical vortices) as shown in **Fig 8(b)**. Smoke is mixed with back part vortices once it is released through chimney at back wall and is reentered into the house via adjoining window. Contaminant air is pulled inside through adjoining window opening due to low pressure inside. In this air movement phenomenon, the extracted smoke from vent pipe reenters into the room causing high indoor air concentration.

It is speared by 68% in leeward side (i.e. back part of house) at opening height 1m near chimney outlet as shown in **Fig 9 (b)**. It is due to high air velocity as hot smoke comes out form ventoutlet.

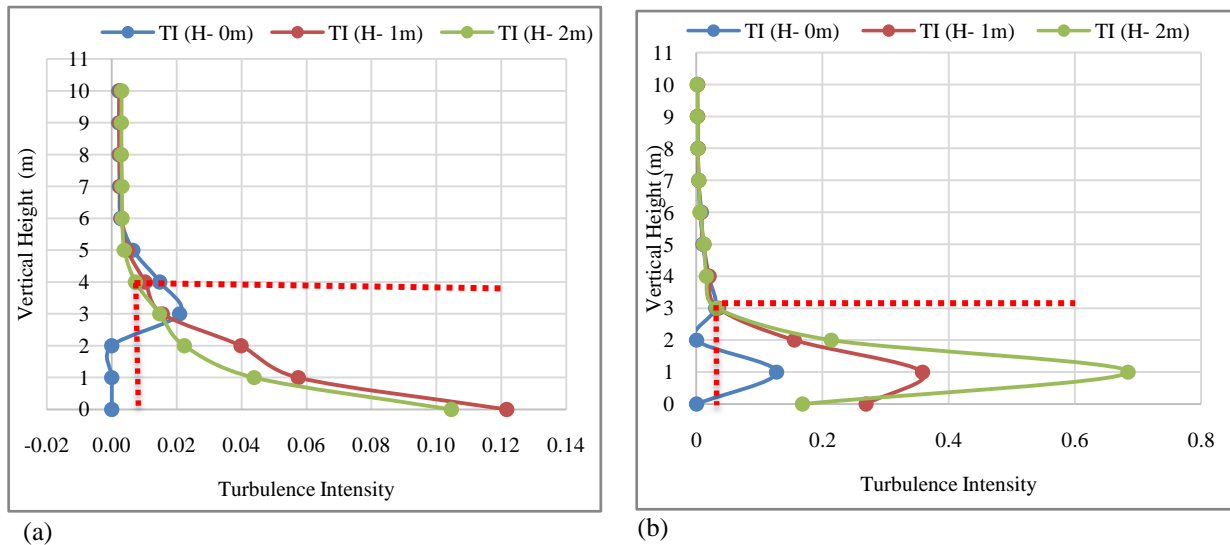


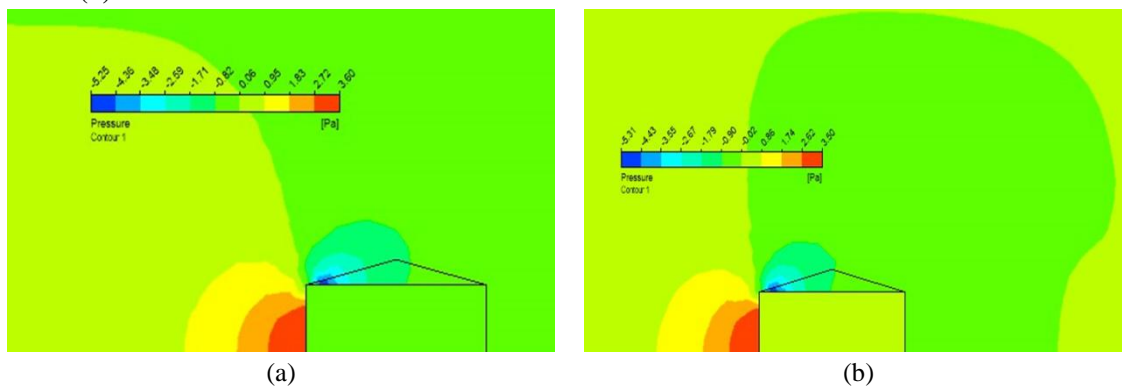
Figure 9: Turbulence intensity distribution: a) turbulence intensity on windward (front part) of house; b) turbulence intensity on leeward side (back part) of house

Pressure distribution along a vertical centerline of windward side, roof and leeward side as shown in Fig.6(b), the location of maximum negative pressure coefficient value for windward side ( $C_{pW}$ ) is found -0.21 at the height of 1m. Location of maximum negative pressure coefficient ( $C_{pL}$ ) with a value of -0.29 is found at a height of 1m from the ground which is leeward vortex point as shown in Fig 8(b). The similar result is found in the study of the formation of horseshoe vortex around cube [32].

Pressure coefficient on the roof ( $C_{pR}$ ) is found -0.46 located at a height of 2.5m. Suddenly decrease in  $C_p$  towards lee side at height 1m (back part of a house) as shown in Fig 6(a) is due to vent outlet nearby.  $C_p$  drops down towards wind side at a height of 2.5m (roof height), this is due to the effect of inclined roof orientation. The result is matched with the result obtained while modeling with low rise building by Goliber, Matthew Robert, 2009 [16].

**3.2.2.2. Wind flow from back side of house**

In a similar way, when the wind blows from the back part of the house towards the front part, it results in the high pressure on a back part of the house and inclined roof and low pressures in the front part of a house. Once smoke is released from the chimney at the height of 1.2m, smoke is immediately carried over the lee side bringing to the ground and then back to the house as depicted in Fig 11(b) due to the formation of a vortex on the leeward side. The smoke reenters into the house via front window and door frequently in unacceptable concentrations as air sucked back into nearby openings due to low pressure as shown in Fig 10(a), 10(b), 10(c) and 10(d).



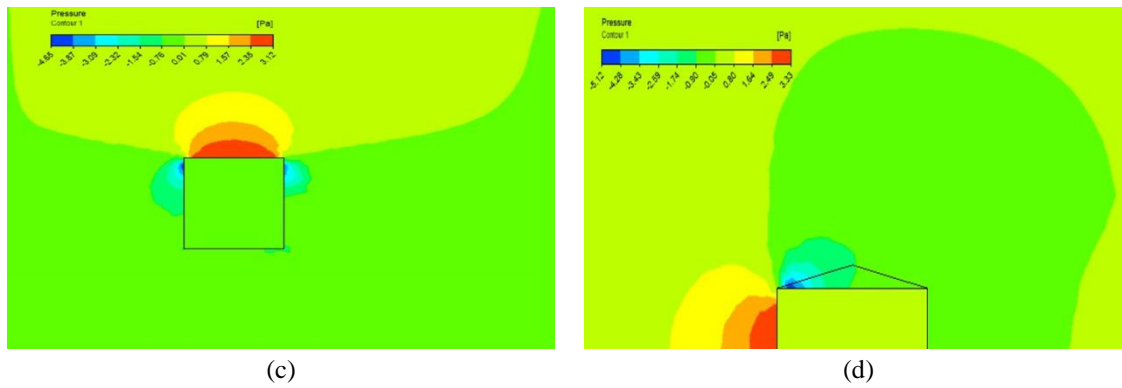


Figure 10: Air flow from back to front part of house- pressure contour: (a) YZ plane front window central plane (b) YZ plane front door central plane (c) XZ plane at chimney height plane (d) YZ back window central plane

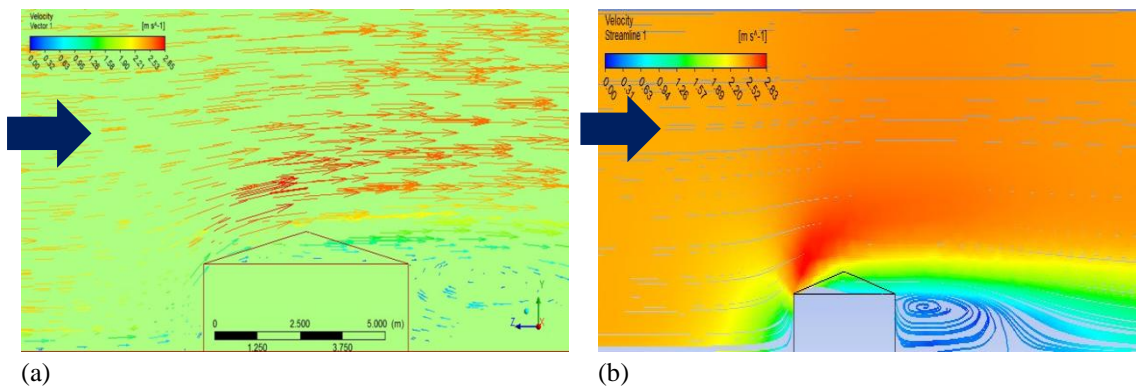


Figure 12: Air flow from back part to front part of the house: (a) velocity vector YZ plane central plane (b) streamline velocity YZ central plane

Smoke from the back part is carried by air towards front part due to a suction effect caused by negative pressure from leeward side. Air with smoke is sucked towards house via door and window openings. Thus, contaminant air reenters into the house immediately after it extracts out from the vent pipe.

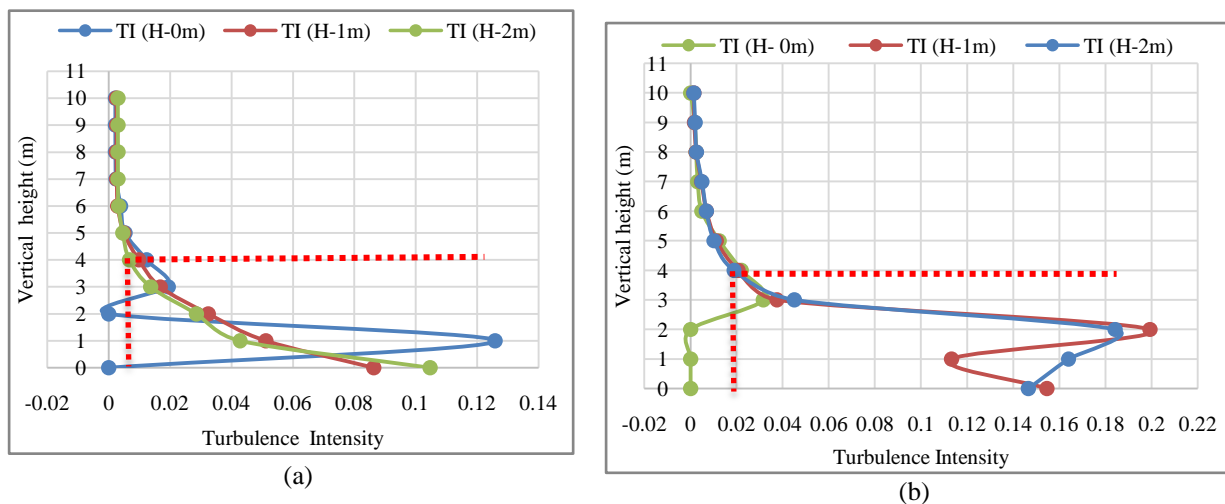


Figure 12: Turbulence intensity distribution: a) turbulence intensity windward side (front part); b) turbulence intensity leeward side (back part)

The high wind velocity causes the friction and turbulence as shown in Fig. 12(a) and 12(b). The air then moves over ground resulting the lowest velocity at ground level and increases with the height and remains almost

constant above 4m as shown in **Fig. 12(a)** and **12(b)**. TI at wind side (back part) at 1m vertical height and 0m horizontal distance is peaked as in **Fig 12(a)**. TI is peaked by 20% at of 2m vertical height and 1m horizontal distance from the house on the leeward side (i.e. front part of the house). The intensity gradually decreases and follows a steady path with the height above the house. The similar result is presented in a study done by Park et al., 2005 [30]. Therefore, it is better to maintain stack height at least above 4m vertical distance from ground level that prevents a problem of backflow.

As per pressure distribution along a vertical centerline of windward side, roof and leeward side as shown in **Fig.6 (b)**, a location of maximum positive CpW with a value of 0.45 is found at the height of 1m from the ground which is the windward vortex point. The pressure coefficient on the roof (CpR) is found as -0.21 at the height of 2m. Maximum negative pressure coefficient value for leeward side (CpL) is obtained as -0.30 at the height 4m from the ground. The excessive rise in Pressure coefficient in wind side (back part of a house) at the height of 1m is due to window opening as shown in **Fig. 7(b)**. The result obtained are closest with result depicted by Richards et al., 2007 [31] with wind-tunnel test and Beyers et al., 2004 [18] with CFD simulation. Hence, IAQ monitoring results of the houses with ICS are found more than safe value. Therefore, air flow from both sides causes backflow towards indoor space resulting IAQ concentration higher than the safe value for a health of dwellers.

#### 4. Conclusion and recommendation

This study has found a higher concentration of IAP in households even using the ICS with chimney. The 8hours average CO and 24hours average PM<sub>2.5</sub> concentration are found 27.11ppm and 825.4 $\mu\text{g}/\text{m}^3$  respectively, which exceeds the safe threshold value. The modeling result depicts the cause of higher pollutants concentration inside a house is due to an effect of backflow with short chimney height of 1.2m. The results show that the pullout smoke via chimney at low height reenters into the house due to high turbulence intensity (TI) i.e. 68% on leeward side while air flow from front to back part of the house and 20% while airflow from back to a front part of the house. This indicates that the current practices of the chimney are the cause of higher concentration of pollutants inside the house. Hence, the effect of backflow is the major problem experienced due to position and orientation of chimney with the short height placed nearby back window opening.

Based on modeling results of this study, it has been recommended for the placement of the chimney height at least above 3m from the ground level to prevent backflow in a low rise and inclined roof houses, which is similar to the minimal chimney height prescribed by chimney height theory. Thus, future research should focus more on a technical aspect of ICS such as Chimney orientation and height to prevent from backflow problem. Consequently, it helps to reduce the pollution concentration inside the house. Hence, it is vital to maintaining minimal height of chimney in an SCH as per the backflow modeling result to maintain IAQ with safe standard value.

#### References

- [1]. Alternative Energy Promotion Center. (2016). National Rural and Renewable Energy Programm (AEPC/NRREP)
- [2]. Anderson, J.D. (1995). Computational Fluid Dynamics. McGraw –Hill, New York; Vol 206.
- [3]. Armendariz –Arnez Cynthia, Rufus Edwards D, Johnson Michael, Rosas I Arma, Masera Omar R, Spinosa F. (2010). Indoor particle size distributions in home with open fires and improved Patsari cookstoves. Atmos. Environment; 44: 2881-6.
- [4]. Arya, S.P. (1999). Air Pollution Meteorology and Dispersion. New York: Oxford University Press.
- [5]. Ashish Singh, Bhushan Tuladhar, Karuna Bajracharya, Ajay Pillarisetti. (2012). Assessment of effectiveness of improved cookstoves in reducing indoor air pollution and improving health of Nepal. Energy for sustainable development, 16, 406 - 414.
- [6]. Berrueta VM, Edwards RD, Masera OR. (2008). Energy performance of wood-burning cookstoves in Michoacan, Mexico. Renew Energy, 33(5):859 - 70.



- [7]. Blocken B, Carmeliet J, Stathopoulos T. (2007). CFD evaluation of wind speed conditions in passages between parallel buildings – effect of wall function roughness modification for the atmospheric boundary layer flow. *J. Wind Eng Ind Aerodyn*, 95:941- 62 doi:10.1016/j.jweia.2007.01.013.
- [8]. Blocken B, Carmeliet J. (2006). The influence of the wind blocking effect by a building on its wind driven rain exposure. *J. Wind Eng Ind Aerodyn*, 94(2): 101 -127.
- [9]. Blocken B, Moomen P, Stathopoulos T, Carmeliet J. (2008). A numerical study of existence of Venturi - effect in passage between perpendicular buildings. *J. Eng Mech- ASCE.*, 134 (12): 1021 - 1028.
- [10]. Blocken B, Stathopoulos T, Carmeliet J. (2008). Wind Environmental Conditions in passages between two long narrow perpendicular buildings. *J. Aerospace Engineering, ASCE*; 21(4): 280-287.
- [11]. Chunzi Nan, Jiming Ma, Zhao Luo, Shuangling Zheng, Zhengwei Wang. (2015). Numerical study on the mean velocity distribution law of air backflow and the effective interaction length of airflow in forced ventilated tunnels. *Tunneling and underground Space Technology*, 46:104 -110.
- [12]. Dhakal Shobhakar. (2008). *Climate Change and Cities: The Making of a Climate Friendly Future*.
- [13]. Dutton AG, Halliday JA, Blanch MJ. (2005). The feasibility of building mounted/integrated wind turbines (BUWTs): achieving their potential for carbon emission reductions. Energy Research Unit, Rutherford Appleton Laboratory, Science & Technology Facilities Council.
- [14]. EPA – Environmental Protection Agency. (2000). "Air Quality Criteria for Carbon Monoxide", EPA 600/P-99/001F, 2.ed, Washington, United States of America, 295.
- [15]. Ezzati M, Kammen DM. (2001). Indoor air pollution from biomass combustion and acute respiratory infections in Kenya: an exposure – response study. *Lancet* ; 358(9287); 619-24.
- [16]. Goliber, Matthew Robert. (2009). Pressure distribution on the roof of a model low-rise building tested in a boundary layer wind tunnel" Graduate Theses and Dissertations, Paper 11103.
- [17]. Hanna, R., Dufflo, E., Greenstone, M. (2012). *Upin Smoke: The Influence of Household Behavior in the Long-Term Impact of Improved Cooking Stoves*. Working Paper. Cambridge Massachusetts. <http://bit.ly/2039004>.
- [18]. J.H.M. Beyers, P.A. Sundsbo, T.M. Harms. (2004). Numerical simulation of three-dimensional, transient snow drifting around a cube. *J. of Wind Eng. and Indus. Aero.*, 92(9): 725 -747.
- [19]. Jerneck, A., Olsson, L. (2012). A smoke free kitchen: initiating community based co- production for cleaner cooking and cuts in carbon emissions. *Journal of Cleaner Production*. <http://dx.doi.org/10.1016/j.jclepro.2012.09.026>.
- [20]. Jiang Y, Chen Q. (2001). Study of natural ventilation in a building by a large eddy simulation. *J. Wind Eng Ind Aerodyn*, 89 (13):1155-1178.
- [21]. Johnson M, Edwards R, Berrueta V, Masera O. (2010). New approaches to performance testing of improved cookstoves. *Environ Sci Technol*, 44(1):368 -74.
- [22]. Kar Abhishek, Rehman Ibrahim H, Jennifer Burney, Praveen Puppala S, , Ramasubramanyaiyer Suresh, Lokendra Singh. (2012). Real time assessment of Black carbon pollution in Indian Households due to traditional and improved biomass cookstoves. *Environ Sci Tech*, 46(5): 2993-3000.
- [23]. Kato, S., Huang, H. (2009). Ventilation efficiency of void space surrounded by buildings with wind blowing over built-up urban area. *Journal of Wind Engineering and Industrial Aerodynamics*, 97: 358 - 367.
- [24]. Lewis, J. J., Pattanayak, S. K., (2012). Who adopts improved fuels and cook stoves? A systematic review. *Environmental Health Perspectives* 120, 637–645.
- [25]. Martinuzzi R, Tropea C. (1993). The flow around surface-mounted, prismatic obstacles placed in a fully developed channel flow (Data Bank Contribution). *Journal of Fluids Engineering*, 115:85 - 92.
- [26]. Murakami S, Mochida A. (1988). 3-D numerical simulation of airflow around a cubic model by means of the k- $\epsilon$  model. *Journal of Wind Engineering and Industrial Aerodynamics*, 31:283 - 303.
- [27]. Nepal living Standard Survey. (2012). Central Bureau of Statistics, National Planning Commission Secretariat; NLSS; 2011/12.



- [28]. P.Z. Gao, S.L. Liu, W.K. Chow., N.K. Fong. (2004). Large eddy simulation for studying tunnel smoke ventilation. *Tunneling and Underground Space Technology*, 19, 577 - 586.
- [29]. Palmer, B., (2012). Clean Cookstoves Draw Support, but They May not Improve Indoor Air Quality. *Ishington Post*.
- [30]. Park, S., Kim, S., Lee, H. (2005). Empirical Model for the Air Pollutant Dispersion in Urban Street Canyons, *Journal of Korean Society of Environmental Engineers*, 27 (8): 852 - 858.
- [31]. Richards PJ, Hoxey RP, Connell BD, Lander DP. (2007). Wind-tunnel modelling of the Silsoe cube. *Journal of Wind Engineering and Industrial Aerodynamics*, 95:1384 - 99.
- [32]. Seeta Ratnam G, Vengadesan S. (2008). Performance of two equation turbulence models for prediction of flow and heat transfer over a wall mounted cube. *International Journal of Heat and Mass Transfer*, 51:2834 - 46.
- [33]. Shrimali, G., Slaski, X., Thurber, M.C., Zerriffi, H. (2011). Improved stoves in India: a study of sustainable business models. *Energy Policy* 39, 7543–7556.
- [34]. Smith KR, Dutta K, Chengappa C, Gusain PPS, Berrueta OM, Victor B. (2007). Monitoring and evaluation of improved biomass cookstove programs for indoor air quality and stove performance: conclusions from the Household Energy and Health Project. *Energy Sustain Dev*, 11(2):5 - 18.
- [35]. Still D, MacCarty N. (2006). The effect of ventilation on carbon monoxide and particulate levels in a test kitchen, Boiling Point. Aprovecho Research Center. Household energy network (HEDON), 52: 24 - 6.
- [36]. Troncoso, K., Castillo, A., Maser, O., Merino, L. (2007). Social perceptions about a technological innovation for fuel woodcooking: case study in rural Mexico. *Energy Policy* 35, 2799–2810.
- [37]. Versteeg, H.K. (1995). An introduction to computational fluid dynamics the finite volume method, 2/E. Pearson Education, India.
- [38]. Wang, F. (2004). *Computational Fluid Dynamics (CFD) software Analysis principle and application*. Tsinghua University Press, Beijing.
- [39]. World Health Organization. (2005). Indoor air pollution from solid fuels and risk of low birth weight and stillbirth. World Health Organization. Johannesburg: WHO Library Cataloguing-in-Publication Data.
- [40]. World Health Organization. (2005a). WHO Air Quality Guideline for Particulate matter, ozone, nitrogen dioxide and sulfur dioxide: air quality guideline global update. Geneva 27, Switzerland, World Health Organization.
- [41]. Wright NG, Hargreaves DM. (2006). Unsteady CFD simulations for natural ventilation. *Int. J Vent*, 5(1), 13-20.
- [42]. Y. Ozmen, E. Baydar, J.P.A.J. van Beeck. (2016). Wind flow over the low – rise building models with gabled roofs having different pitch angles. *Building and Environment*. 95, 63-74.
- [43]. Yang Y, Gu M, Chen S, Jin X. (2009). New inflow boundary conditions for modelling the neutral equilibrium atmospheric boundary layer in computational wind engineering. *Journal of Wind Engineering and Industrial Aerodynamics*. 97, 88- 95.

